Journal of Associated Medical Sciences 2022; 55 (3): 26-35

JAMS
Journal of Associated Medical Sciences

Thai-Journal Citation Index Centre (TCI) & ASEAN Citation Index (ACI)

Journal of Associated Medical Sciences

Journal homepage: https://www.tci-thaijo.org/index.php/bulletinAMS/index

Evaluation of the Varian TrueBeam™ 6 MV phase-space files for the Monte Carlo simulation in small field dosimetry

Mananchaya Vimolnoch[1,2*] Isra Israngkul Na Ayuthaya[2] Sakda Kingkaew[2] Sornjarod Oonsiri[1,2]

[1]Medical Physics Program, Department of Radiology, Faculty of Medicine, Chulalongkorn University, Bangkok, Thailand.
[2]Division of Radiation Oncology, Department of Radiology, King Chulalongkorn Memorial Hospital, Bangkok, Thailand.

ARTICLE INFO

Article history:
Received 22 February 2022
Accepted as revised 16 June 2022
Available online 5 July 2022

Keywords:
Small field, phase-space file, Monte Carlo simulation

ABSTRACT

Background: The Monte Carlo (MC) simulation is an effective tool for determining the absorbed dose in small field sizes. To calculate accurate results, the MC simulation requires precise geometric and material descriptions of the linear accelerator head. Due to proprietary information issues, the description of the Varian TrueBeam™ linear accelerator (Varian Medical Systems, Palo Alto, CA) head geometry and material information are not available. Instead, the manufacturer provided a phase-space file just above the jaw for each photon energy level. Although several studies have validated the accuracy of this phase-space file, to the best of our knowledge, there are no reported data for a small field size (<2x2 cm^2) of 6 MV photon beams.

Objectives: The purpose of this study was to evaluate the Varian TrueBeam™ phase-space file of the 6 MV photon beam provided by the manufacturer for the Monte Carlo (MC) simulation in small field dosimetry.

Materials and methods: The TrueBeam™ linear accelerator was simulated using an EGSnrc MC code with a Varian phase-space file as the input. The simulation was compared with the measurement using percent depth dose (PDD) and beam profile, and the field output factor (FOF) for the 0.6x0.6, 1x1, 2x2, 3x3, 4x4, 6x6, and 10x10 cm^2 field sizes.

Results: The agreement between the measurements and simulated PDD data was under 2.2% beyond the buildup region. The distance to agreement (DTA) in the buildup region was within 1.0 mm. The simulation data presented identical profiles with the measurement within 1.0% of the dose difference or 1.2 mm of the DTA. The mean dose difference in the radiation field was ≤1.5% for the ≥1x1 cm^2 field size. The largest deviation was observed in the 0.6x0.6 cm^2 inline beam profile. The deviation of the penumbra and full width at half maximum (FWHM) between simulation and measurement was <2 mm. The agreement of the simulated and measured FOF was within 1.0%, except for the 0.6x0.6 cm^2 field size.

Conclusion: Overall, the MC simulation demonstrates data that is consistent with the measurement for the ≥1x1 cm^2 field sizes. These data assure that the 6 MV Varian phase-space file can be used as a radiation source for accurate MC dose calculation in a small field. However, a large discrepancy in beam profiles was observed at the 0.6x0.6 cm^2 field size due to the different primary source sizes among Truebeam™ machines.

* **Corresponding author.**
Author's Address: *Medical Physics Program, Department of Radiology, Faculty of Medicine, Chulalongkorn University, Bangkok, Thailand.*
** **E-mail address:** vmananchaya@gmail.com
doi: 10.12982/JAMS.2022.021
E-ISSN: 2539-6056

Introduction

Recent advanced techniques in photon beam radiotherapy have been developed to improve the accuracy of radiation delivery while still allowing for shorter treatment times. These advances have led to an increased use of small fields over the past decades.[1] However, accurate dose measurement in small fields is challenging due to its three conditions. The first condition is the lack of lateral electronic equilibrium (LCPE) that occurs when the size of the field becomes smaller than the range of the lateral charged particle equilibrium (r_{LCPE}). Source occlusion also occurs in small fields as a second condition, resulting in an overlapping of the penumbra. Both conditions are responsible for a sharp drop in beam output. The third condition is associated with the detector for a given field size. These detector aspects include the volume averaging around high-gradient dose distributions and the fluence/dose perturbations due to the different physical densities between the detector and medium.

In 2017, the International Atomic Energy Agency (IAEA) along with the American Association of Physicists in Medicine (AAPM) published Technical Reports Series #483 (TRS 483)[1] that provides a code of practice (CoP) for small field dosimetry. The CoP defines the field output factor $(\Omega_{Q_{clin},Q_{msr}}^{f_{clin},f_{msr}})$ as the ratio of absorbed dose to water in the clinical field $(D_{Q_{clin}}^{f_{clin}})$ and the absorbed dose to water in the machine-specific reference field $(D_{Q_{msr}}^{f_{msr}})$. The equation for field output factor is:

$$\Omega_{Q_{clin},Q_{msr}}^{f_{clin},f_{msr}} = \frac{D_{Q_{clin}}^{f_{clin}}}{D_{Q_{msr}}^{f_{msr}}} \quad \text{Eq.1}$$

In large clinical fields, the field output factor has commonly been approximated by the ratio between detector readings in the clinical field $(M_{Q_{clin}}^{f_{clin}})$ and reference field $(M_{Q_{msr}}^{f_{msr}})$ because the stopping-power ratios and perturbation correction factors are normally constant with field size. For small fields, this condition no longer holds. TRS 483 has recommended the field output correction factor $(k_{Q_{clin},Q_{msr}}^{f_{clin},f_{msr}})$ to account for the differences in the response of a detector in the clinical and reference fields. The equation then becomes

$$\Omega_{Q_{clin},Q_{msr}}^{f_{clin},f_{msr}} = \left(\frac{M_{Q_{clin}}^{f_{clin}}}{M_{Q_{msr}}^{f_{msr}}}\right) \times k_{Q_{clin},Q_{msr}}^{f_{clin},f_{msr}} \quad \text{Eq.2}$$

Another approach to determine the absorbed dose is the Monte Carlo (MC) method, which has been found to be an effective tool in overcoming the challenges of small field dosimetry. The MC can simulate the scenario of the radiation transport to calculate the accurate deposited dose when measurement is not possible.[2] Many recent studies have used the MC simulation to examine the field output correction factors of small field sizes.[3-5] To calculate accurate results, the MC simulation requires precise geometric and material descriptions of the linear accelerator head. Due to proprietary information issues, the description of the Varian TrueBeam™ linear accelerator (Varian Medical Systems, Palo Alto, CA) head geometry and material information upstream of the jaw are not available. Instead, the Varian MC research team provided a phase-space file just above the jaw for each photon energy level. This phase-space file can be used as source to transport particles through the geometry of the jaws, and other beam modifiers, for calculating the absorbed dose. The Varian phase-space file was generated using GEANT4 MC code with the Varian TrueBeam™ head schematics imported from the computer-aided design as the input.[6] The first version of the phase-space file was stored in a cylindrical space that cannot be used by the BEAMnrc MC code that requires the planar format. Varian subsequently released the second version of the phase-space file that was stored on a flat surface.

Although several studies have validated the accuracy of this phase-space file, to the best of our knowledge, there are no reported data for the 6 MV photon beam field sizes smaller than 2x2 cm^2.[6-11] The primary photon source width strongly affects the beam profiles of small fields due to the source occlusion effect. The source size of the TrueBeam™ machine varies between 1.0-1.5 mm.[12] Thus, It cannot be assumed that this universal phase-space file will produce an accurate dose distribution for small fields.

This study compares the dosimetric characteristics of the measured Varian TrueBeam™ 6 MV small photon beams with the MC simulation using the version 2 phase-space data available from the manufacturer. The simulation was compared with the measurement using percent depth dose (PDD), beam profile, and field output factor (FOF) as a function of jaw setting.

Materials and methods

All simulations and measurements were performed on a Varian TrueBeam™ linear accelerator using 6 MV photon beam energy.

Monte Carlo simulation

The EGSnrc code system,[13] user codes BEAMnrc,[14] and DOSXYZnrc[15] were used for the MC simulations. Each simulation consisted of three steps. First, BEAMnrc was used to simulate the particle transport through the components of the linear accelerator treatment head. Second, DOSXYZnrc was used to compute the dose deposited within the water phantom. Finally, the obtained results were compared with the measured data.

The Varian TrueBeam™ version 2 phase-space file of the 6 MV photon beam energy was adopted from the MyVarian website (https://www.myvarian.com).[6] This phase-space file contains information about the radiation interactions within the linear accelerator treatment head, such as the position, energy, directionality, and type of each particle. The phase-space file was then used as the radiation source in BEAMnrc. The data for the material and geometry of the linear accelerator components below the phase-space plane were taken from the Varian TrueBeam™ Monte Carlo package version 1.1 available on the MyVarian website. Figure 1 presents the schematics of the linear accelerator model simulations by BEAMnrc. The Varian phase-space file was located above the Y jaw at 26.7 cm from the source. Only the X and Y jaws were modeled using JAWS CM. The slab of air

was created after the X jaw using SLABS CM at a distance of 100 cm from the source. The particles that reached the end of the air slab were stored in the second phase-space file. These field size-specific phase-space files were used as an input source for the subsequent water phantom simulation in DOSXYZnrc. The number of histories ranging from $1x10^9$-$4x10^{10}$ was simulated with BEAMnrc transporting the particles from the location of the Varian phase-space file. The global ECUT and PCUT was 0.521 MeV and 0.01 MeV, respectively. The particles with total energies below these values were terminated with the energy deposited in the current voxel. No variance reduction techniques were used. The default EGSnrc transport parameters were applied in the simulation.

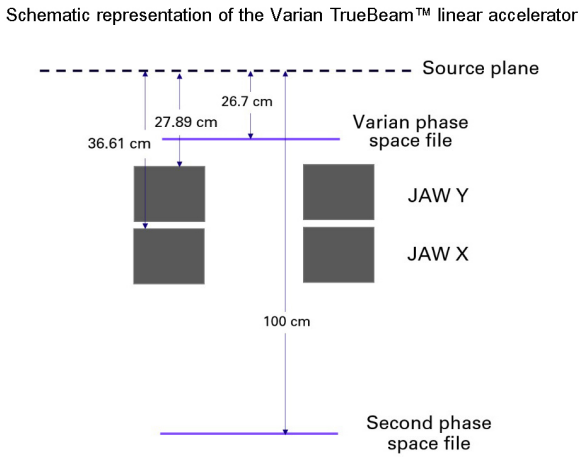

Figure 1. *Schematic representation of the Varian TrueBeam™ linear accelerator model.*

The MC methodology was evaluated by comparing the simulated PDD, beam profile, and FOF with the measurements. This process used nominal field sizes of 0.6x0.6, 1x1, 2x2, 3x3, 4x4, 6x6, and 10×10 cm^2 for the jaw-collimated fields.

To calculate the three-dimensional dose distributions in a virtual water phantom, a 30x30x30 cm^3 water phantom was generated using DOSXYZnrc. The voxel sizes were between 0.1 x 0.1 x 0.5 cm^3 and 0.5x0.5x0.5 cm^3. The voxel resolution varied according to the field size to obtain accurate penumbra data. A large enough number of histories were selected for each simulation to keep the statistical uncertainty less than 0.5% at the maximum dose voxel and 0.7% for all the voxels inside the radiation field.

The output files that contain the dose deposited in each voxel per number of particles and the associated statistical uncertainty were created using the DOSXYZnrc code. These files were exported to MATLAB (The MathWorks, Natick, MA) to calculate the dosimetric quantities. The PDDs and beam profiles were normalized so that a comparison between the MC simulation and the measurements could be done. To calculate the PDD, the dose scoring in voxels along the central beam axis was normalized to the dose at d_{max}. The simulated beam profile was determined by normalizing the voxel dose at 10 cm depth to the dose on the central axis.

Measurements

Percentage depth doses and beam profiles

The PDDs, crossline profiles, inline profiles, and FOFs were acquired in a 3D water scanning system (Blue Phantom2, IBA Dosimetry, Memphis, TN) with OmniPro-Accept software. The experiments were set at 100 cm SSD. The PDDs for the 6x6 and 10x10 cm^2 fields were measured using IBA CC13 (IBA Dosimetry, Schwarzen-Bruck, Germany). For field sizes smaller than 6x6 cm^2, the Sun Nuclear EDGE detector (Sun Nuclear Corporation, Melbourne, FL) was used. The measured crossline and inline beam profiles were obtained using the Sun Nuclear EDGE detector scanning across the field area at a depth of 10 cm. Similar to the MC simulation, the depth-dose curves were normalized to the maximum dose depth to calculate the PDD of each field size. The beam profiles were normalized to 100% at the central axis to their corresponding field size.

Field output factors

The FOFs at the 10 cm depth were measured using the IBA CC01, Sun Nuclear EDGE, and PTW 60003 natural diamond (PTW, Freiburg, Germany) detectors. These detectors were recommended by TRS 483 for small field dosimetry. The characteristics and description of the detectors used in this study are presented in Table 1. The IBA CC01 and Sun Nuclear EDGE detectors were set perpendicular to the central beam axis. Both detectors were positioned at the center of the radiation beam using crossline and inline scans to find the position of the maximum signal according to the TRS 483 guidelines. The natural diamond detector was vertically positioned and aligned at the center of the light field crosshair of the 1x1 cm^2 field. The IBA DOSE-1 electrometer was connected to each detector to measure the collected charge.

Table 1 Resistive load and training volume for inspiratory muscle traning of each participant.

Type	Model	Active volume	Active volume dimensions	Application
Cylindrical Ionization chamber	IBA CC01	10 mm^3	Ø 2 mm x l 3.6 mm	Field output factors
	IBA CC13	130 mm^3	Ø 6 mm x l 5.8 mm	PDDs≥6x6 cm^2
Shielded diode	Sun Nuclear Edge	0.019 mm^3	Square 0.8 mm x 0.8 mm thickness 0.03 mm	PDDs<6x6 cm^2 Beam profiles Field output factors
Natural diamond	PTW 60003 natural diamond	1.2 mm^3	Disk, Ø 2.3 mm thickness 0.28 mm	Field output factors

The FOFs in this study are defined in Eq.3. The ratio of the detector reading normalized to the 10x10 cm^2 reference field was multiplied by the field output correction factors (k). These k factors were taken from Table 26 of TRS 483 except for that for the Sun Nuclear Edge detector at the 0.6x0.6 cm^2 field size. This is because the protocol provides the k factor of Sun Nuclear Edge only for field sizes ≥0.8x0.8 cm^2.

$$FOF = \frac{\text{Chamber reading at any field size}}{\text{Chamber reading at 10×10 cm}^2} \times k \text{ (TRS 483)} \quad \text{Eq.3}$$

The S_{clin} was determined for selecting the k factors. The S_{clin} is defined by the full width at half maximum (FWHM) of the beam profile and given by

$$S_{clin} = \sqrt{A.B} \quad \text{Eq.4}$$

where A and B is the crossline and inline FWHM, respectively, at the 10 cm depth, determined from the beam profile measured with the Sun Nuclear EDGE detector.

Results

Percentage depth doses

To compare the simulated and measured PDD data, two different evaluation parameters were considered: the dose difference in the region beyond d_{max} and the distance to agreement (DTA) in the buildup region. The dose difference was defined as the percentage difference of the simulated to the measured dose. The DTA is the distance between a measurement and the MC calculation point with the same absorbed dose[16]. The percentage depth dose curves of the 6 MV photon beam are plotted in Figure 2 for the 10x10, 6x6, 4x4, 3x3, 2x2, 1x1, and 0.6x0.6 cm^2 field sizes delivered at 100 cm SSD. The differences between the simulation and measurement are described below.

In a region deeper than the maximum dose (>1.5 cm), the measurement and MC simulation data closely agreed with a dose difference of less than 2.2%, while the mean dose differences were less than 1.0% for all field sizes. The mean dose difference ± standard deviation between the simulated and measured PDDs beyond the buildup region are reported in Table 2. The absolute value of the dose difference was taken before finding the mean value. In the buildup region, the maximum deviation was found up to 8%. Because the buildup region is a high dose gradient region, small spatial shifts between the measurement and MC dose distribution can result in a high dose difference. When the DTA was analyzed in the buildup region, we found a 1.0 mm agreement between the MC produced PDD and the measurement. Further comparison of the PDD at a 10 cm depth (PDD_{10}) and PDD at a 20 cm depth (PDD_{20}) for simulation and measurement is also presented in Table 2. The maximum difference was ~1.0% for PDD_{10} and PDD_{20}.

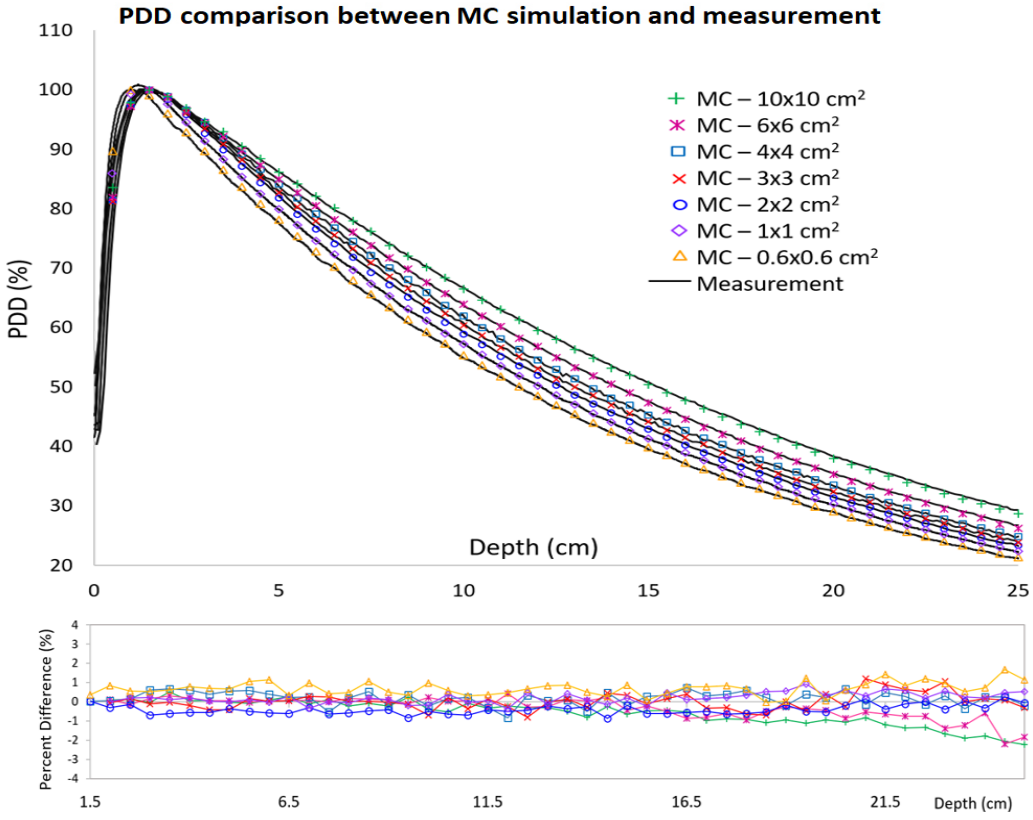

Figure 2. *Percent depth dose curves for all field sizes. Measurements are plotted as solid lines, and the Monte Carlo data are plotted as points. Percent differences between the simulation and measurement are presented in the lower panels.*

Table 2 The mean dose difference and standard deviation of PDDs between simulation and measurement beyond the buildup region. The comparison of PDD at 10 cm and PDD at 20 cm are reported.

Field size (cm^2)	Mean dose difference (%) ±SD	PDD_{10}			PDD_{20}		
		MC	Measured	%diff	MC	Measured	%diff
10x10	0.6±0.6	66.4	66.2	-0.4%	38.0	38.3	0.9%
6x6	0.4±0.5	63.9	63.8	-0.2%	35.3	35.4	0.4%
4x4	0.4±0.2	62.0	62.1	0.2%	33.5	33.4	-0.2%
3x3	0.3±0.3	60.3	60.7	0.7%	32.4	32.3	-0.4%
2x2	0.4±0.2	58.9	59.2	0.5%	31.3	31.5	0.5%
1x1	0.3±0.2	57.2	57.3	-0.2%	30.3	30.3	0.3%
0.6x0.6	0.7±0.4	55.3	54.8	-1.0%	29.0	29.0	-0.1%

Beam profiles

For the dose profiles, the crossline and inline directions were considered. Figure 3 presents the normalized measured and simulated half-profiles for all field sizes at the 10 cm depth. To evaluate the beam profile, the dose difference was analyzed in the radiation field region (within 80% of the normalized dose). The agreement between the simulation and measurement in the shoulder and penumbra region (beyond the in-field region) was evaluated by determining the DTA. Table 3 demonstrates the dose differences inside the radiation field between the measurement and simulation. The mean dose difference was less than or equal to 1.5% for field sizes ≥1x1 cm^2. For field sizes ≥4x4 cm^2, the deviation was within 1.5% for more than 97% of the points in the radiation field region. For field sizes ≤3x3 cm^2, a large deviation was observed. The mean dose differences were found up to 5.0% for the 0.6x0.6 cm^2 field size. The pass rate (the point displaying a percent difference of ≤1.5%) in the radiation field region was 78%, 75%, and 67% for the crossline profile of the 2x2, 1x1, and 0.6x0.6 cm^2 field, respectively. For the inline profile, the pass rate was 81%, 75%, and 17% for the 2x2, 1x1, and 0.6x0.6 cm^2 field, respectively. The discrepancy between the simulation and measurement was also found in the profile shoulders. In the small field, the profile exhibited a very steep dose gradient, and the flattened region was less than 80% of the normalized dose. Therefore, the DTA was applied to evaluate every point of the 0.6x0.6, 1x1, and 2x2 cm^2 fields. The DTA of the region where the dose difference exceeded 1.0% was less than 1.0 mm and 1.2 mm for all crossline and inline profiles, respectively.

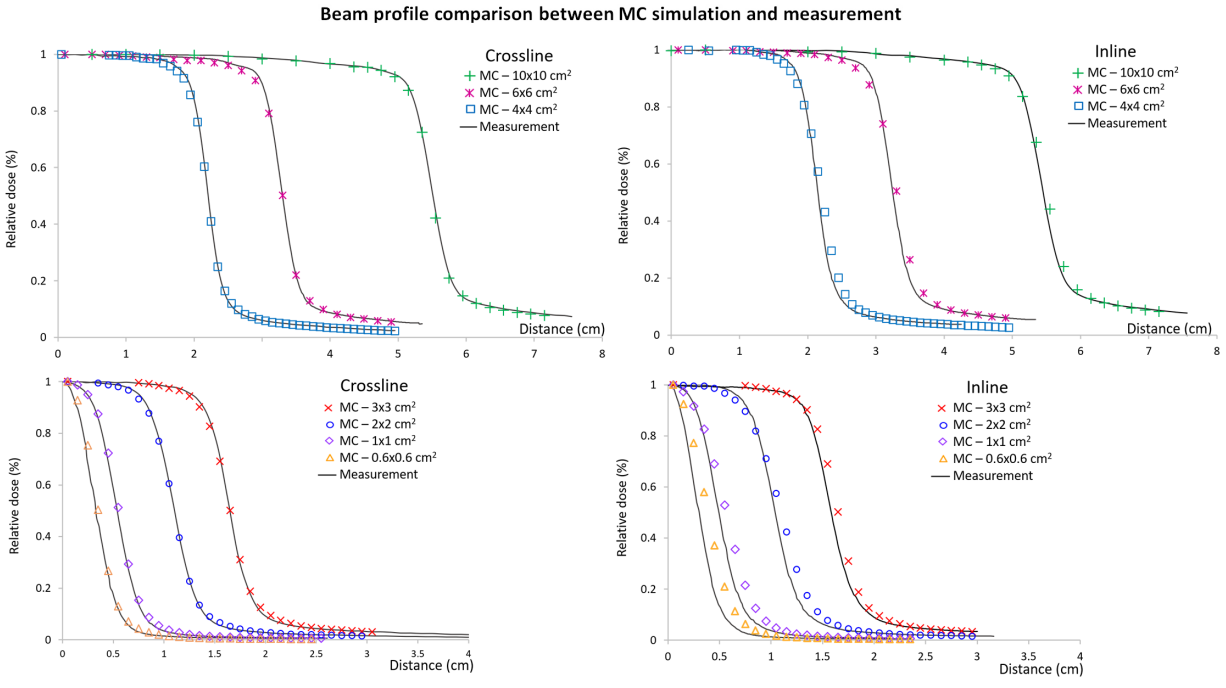

Figure 3. *Crossline (left) and inline (right) half profiles for the 10x10, 6x6, 4x4, 3x3, 2x2, 1x1, and 0.6x0.6 cm^2 field sizes. Measurements are plotted as continuous lines, and the Monte Carlo data are plotted as points.*

Table 3 Percent difference of the beam profiles between Sun Nuclear Edge measurement and MC simulation inside radiation field. The DTA of the region where the dose difference exceeds±1% is shown.

Field size (cm^2)	Crossline profile		Inline profile	
	Mean dose differences (%)±SD	DTA (mm)	Mean dose differences (%)±SD	DTA (mm)
10x10	0.2±0.2	<1.0	0.3±0.2	<1.0
6x6	0.7±0.4	<1.0	0.4±0.3	<1.0
4x4	0.5±0.4	<1.0	0.4±0.4	<1.0
3x3	0.5±0.5	<1.0	0.3±0.2	<1.0
2x2	0.7±0.7	<1.0	0.9±0.9	<1.2
1x1	0.6±0.7	<1.0	1.5±1.4	<1.1
0.6x0.6	4.9±3.6	<1.0	5.4±3.6	<1.2

Other profile characteristics, the FWHM and penumbra, were evaluated. The results are summarized in Table 4. The FWHM was determined from a distance of 50% relative dose and the penumbra was defined as the region between 20% and 80% of the central axis dose. As seen in Table 4, the simulated FWHM agrees with the measurement within 1.5 mm for the field sizes >0.6x0.6 cm^2. The deviation of the penumbra was also within 1.5 mm for all field sizes. Overall, the FWHM and penumbra widths tended to be larger than the measurement in the inline direction, with the differences increasing with the decreasing field size. However, the differences did not exceed 2.0 mm.

Field output factors

The comparison of the FOFs between the MC simulation and measurement for field sizes ranging from 0.6×0.6 cm^2-10×10 cm^2 are given in Table 5. Excellent agreement between the MC simulation and measurement was found within 1.0%, except for the 0.6x0.6 cm^2 field, where the maximum difference was 2.2% obtained by the IBA CC01 detector. The FOF of the 0.6x0.6 cm^2 field measured by the Sun nuclear EDGE detector was omitted because no correction factor was provided by TRS 483.

Table 4 Comparison of simulated and measured FWHM (distance between 50% isodose level) and penumbra width (distance between 20% and 80% isodose level) for all field sizes.

Field size (cm^2)	Crossline (mm)						Inline (mm)					
	FWHM width			Penumbra width			FWHM width			Penumbra width		
	MC	Measured	Deviation	MC	Measure	Deviation	MC	Measured	Deviation	MC	Measure	Deviation
10x10	110.0	110.1	0.1	5.3	5.5	-0.2	110.0	108.9	1.1	6.5	5.6	1.0
6x6	66.0	66.0	0.0	4.6	4.3	0.3	66.1	64.9	1.2	6.0	4.6	1.4
4x4	44.1	43.9	0.2	4.0	3.6	0.4	44.1	42.9	1.2	5.0	3.8	1.2
3x3	33.0	32.9	0.1	3.7	3.4	0.3	33.1	31.7	1.4	4.9	3.8	1.1
2x2	22.0	22.0	0.0	3.6	3.5	0.1	22.0	20.8	1.2	4.6	3.5	1.1
1x1	11.1	10.8	0.3	3.2	3.2	0.0	11.3	9.9	1.4	4.0	3.1	0.9
0.6x0.6	7.0	6.6	0.4	2.8	2.9	-0.1	7.7	6.0	1.7	3.3	2.7	0.6

Table 5 Field output factors of 6 MV using IBA CC01, Sun Nuclear EDGE, and PTW natural diamond compare with simulated FOF. The corrections were based on TRS 483 except for 0.6x0.6 cm^2 field size measured with Sun Nuclear EDGE where the correction factor is not provided by TRS 483.

Field Size (cm^2)	Field output factors						
	Simulation	EDGE	%Diff	Diamond	%Diff	CC01	%Diff
6x6	0.923	0.919	-0.4	0.918	-0.5	0.919	-0.4
4x4	0.867	0.862	-0.6	0.862	-0.6	0.864	-0.4
3x3	0.833	0.829	-0.5	0.829	-0.5	0.831	-0.3
2x2	0.795	0.791	0.5	0.790	-0.6	0.790	-0.6
1x1	0.683	0.690	0.9	0.683	0.0	0.679	-0.6
0.6x0.6	0.490	-	-	0.485	-1.0	0.479	-2.2

Discussion

The present study evaluated the MC simulation using the Varian phase-space file version 2 of the 6 MV photon beam for small field dosimetry. The MC simulation and measurement PDDs, beam profiles, and FOFs were compared. Overall, the MC simulation provided data that was consistent with the measurement. The agreement between all measured and MC simulated PDDs data in this study was under 2.2% beyond the buildup region. Large differences were found in the deeper depths (>25 cm) of the PDD where the MC simulation overestimated the dose compared with the measurement data. Our results agree with those of Bergman *et al.*,[9] who simulated the dose distribution of the 6 MV photon beam using a Varian phase-space file. In their study, a maximum deviation of 2% between the simulated and measured PDD for field sizes 2 × 2 cm^2-40 × 40 cm^2 was reported. In another study by Cheng *et al.*,[17] they reported a maximum dose difference of 1.5% for the PDD of a 10x10 cm^2 field. These studies, as well as ours, found that the maximum deviation was in the distal region of the PDD. In addition, an increasing discrepancy between the measured and simulated PDD with depth was observed in many reports[7-10, 18] that evaluated the Varian phase space file. A possible explanation for the discrepancy in the deeper depth region might be the differences in the primary beam energy of the phase-space file and the Varian TrueBeam™ machine in the experiment.[7,19]

The comparison of our simulated PDD_{10} and PDD_{20} with other Varian TrueBeam™ data[20-23] is summarized in Table 6. Our MC results agree within 1.0% for all the compared linear accelerators for the 3x3–10x10 cm^2 field sizes. In addition, the simulated PDD_{10} values fall within the range of those reported by Mamesa[23] who measured the PDDs of small fields using several detectors.

Table 6 Summary of the PDD parameters of 6 MV photon beam from MC simulation (this study) and measured data from previous studies. Measured PDD10 from Mamesa *et al*. were estimated from Figure 1. reported in their paper.

Field sizes (cm^2)	PDD_{10}					PDD_{20}	
	MC (this study)	Glide-Hurst *et al.*[20]	Bayer *et al.*[21]	Chang *et al.*[22]	Mamesa *et al.*[23]	MC (this study)	Chang *et al.*[22]
10x10	66.4	66.2	66.1	66.3	-	38.0	38.1
6x6	63.9	-	-	63.5	63.2 - 64.4	35.3	35.1
4x4	62.0	-	61.4	61.4	61.0 - 62.0	33.5	33.3
3x3	60.3	-	-	60.3	59.6 - 60.8	32.4	32.4
2x2	58.9	-	-	-	58.0 - 59.6	31.3	-
1x1	57.2	-	-	-	56.0 - 58.4	30.3	-
0.6x0.6	55.3	-	-	-	-	29.0	-

For the dose profile, small differences were observed between the measurement and simulation in the in-field dose area for field sizes ≥3x3 cm^2. The DTA of the region where the absolute difference exceeds 1.0% was less than 1.2 mm. Therefore, the simulated data demonstrated identical profiles with the measurement within 1.0% of the dose difference or 1.2 mm of DTA. The FWHM of the 10×10 cm^2 field at the 10 cm depth was similar to that described by Chang[22] with a difference of 0.7 mm. However, our simulated FWHM was 2.0 mm smaller than that reported by Glide-Hurst *et al.*[20] and Beyer *et al.*[21]. These differences were due to the volume averaging effect of the detector used for the beam profile scanning. The Glide-Hurst and Bayer studies used an IBA CC13 detector to measure the profile data, whereas the beam profiles were measured with an IBA SFD diode detector in Chang's study. The large active volume of the detector can lead to inaccurate field edge measurements where a steep dose gradient exists. The previous literature also reported that the FWHM measured using the IBA CC13 detector was 1.8 mm larger than that measured by the Sun Nuclear EDGE detector for the 10x10 cm^2 field.[24] Besoli *et al.*,[7] who validated the Varian phase-space file of the 6FFF MV beam, found that the simulated penumbra was more similar to the diode measurement. Our study used a Sun Nuclear Edge detector to measure the beam profile. Thus, the measured and simulated penumbra and FWHM results agreed within 2.0 mm for all field sizes. The profile data of the field sizes ranging from 1x1 cm^2-6x6 cm^2 were reported by Mamesa *et al.*[23] and the difference in FWHM was less than 2.0 mm compared with our MC results.

The discrepancy between the measurement and simulation in the inline profile was higher than the crossline profile. The widening of the simulated inline profile was observed as the field sizes decreased. Beam profile deviations were also observed for field sizes ≤3x3 cm^2 in other studies.[8, 9, 18] A possible reason for the discrepancy might be partly ascribed to the difference in the primary photon source width among the Varian TrueBeam™ linear accelerators, which were in the range of 1.0-1.5 mm.[12, 25] Pervious studies have found that the dose profile of a small field (<1x1 cm^2) was strongly dependent on the primary photon source size. Cranmer-Sargison *et al.*[25] reported that the dosimetric field widths increased as the source size increased. This is due to the partial source occlusion by the collimated jaw and is markedly affected by the upper jaws because it is closer to the source than the lower one. The slight deviation in the profile shoulder region between the MC and measurement is also explained by the difference in the source size. Because the Varian phase-space

file was scored above the collimator jaw, the user cannot change the primary photon source parameters, such as the energy, angular spread, and diameter. Therefore, it is not possible to fine tune the beam model to better match a specific linear accelerator. This could be crucial issue in a very small field (<1x1 cm^2) when the beam profile is highly dependent on the primary source size and source occlusion effect.

It should be noted that no corrections were made for the PDD and beam profile measurements in this study. The accuracy of the small field measurement by the Si-based diode detector was reported by Francescon *et al*.[26] The variation of the field output correction factor of the diode detector as a function of depth and distance from the central axis for PDD and beam profile measurements was reported in the literature. The beam profile in water measured with the diode detector yielded accurate results up to the penumbra region, but meaningfully underestimated the dose in the tail region where the field output correction factor was increased. Similar results were found by Papaconstadopoulos *et al*.[27] where the diode detector demonstrated minimal deviations within the radiation field. In contrast, significant corrections were observed at the gradient and the low-dose region of the profile. However, the error in the gradient and tail region of the beam profile is not clinically meaningful, because it is considered a very low dose area.[26] Dwivedi[28] reported that the variation of the beam profile measured by the Sun Nuclear Edge detector for field sizes ranging from 0.6x0.6 cm^2-6x6 cm^2 was less than 0.5 mm in FWHM compared with EBT3 radiochromic films (Ashland Inc., Wayne, NJ, USA). Although the Sun Nuclear Edge detector exhibits the correction factor >5% at all depths as reported by Francescon *et al*., other studies[28, 29] demonstrated that the PDD at the fall-off region measured by the Sun Nuclear Edge detector for field size ≤1x1 cm^2 was comparable with other detectors that have been recommended to avoid the need to correct the PDD, such as EBT3 film and the PTW microdiamond detector.[30]

For the FOF measurements, the Sun Nuclear Edge detector exhibits the overresponse FOFs for field size smaller than 2x2 cm^2 due to the scatter from the high density encapsulating material of the detector.[31-33] In contrast, the IBA CC01 and PTW natural diamond detectors were influenced by volume averaging effects that underestimated the FOFs.[10, 34] However, this effect becomes less critical for the PTW natural diamond detector due to the smaller size of the active volume. In addition, the PTW natural diamond detector measurement values were very consistent with the MC values, only deviating ≤1.0%. The difference in FOFs between the measurement and the 6 MV Varian phase-space file in the present study agrees well with previous studies by Constantin *et al*.[6] and Bergman *et al*.[9] However, the smallest field sizes in these studies were limited to 4x4 cm^2 and 2x2 cm^2. The data for comparison obtained using the 6 MV Varian phase space file for field sizes <2x2 cm^2 are scarce, only Gete *et al*.[8], who evaluated the 6FFF phase-space file, have reported the FOF for the 1x1 cm^2 field. In our study, the simulated FOF fell within 2.2% of the measured FOF for all field sizes. This is better than that reported by Gete *et al*.[8] where a deviation of 2.9% was found between the IBA CC01 detector and the simulated output factor of the 1x1 cm^2 field, whereas the deviation was less than 1.0% in our study. However, no correction factor was applied in Gete *et al*.,[8] because the TRS 483 was not published at the time of their study. The output factors of small fields cannot be accurately approximated as the ratio of the detector readings as it is usually done for broad beams. Many studies have reported that the deviation of the field output factors reduced significantly when the field output correction factors based on TRS 483 were implemented.[23, 35, 36] A further comparison with previous studies is presented in Table 7. The agreement was within 1.0% compared with Mamesa *et al*.[23] for the 1x1 cm^2-10x10 cm^2 field sizes. The FOFs taken from Mamesa's study were averaged between the IBA CC01, IBA EFD, and IBA PFD detectors. Casar *et al*.[37] also reported the FOFs that were determine by fitting the signal of the EBT3 radiochromic films and the W1 plastic scintillator (Standard Imaging, Middleton, WI, USA) using an analytical function. A 90 cm SSD was used in their study, making a direct comparison with our results difficult. However, the difference was ~1.6% compared with our MC results.

Table 7 Comparison of field output factors between our MC simulation and measured data from previous studies.

Field size (cm^2)	MC (this study)	Mamesa *et al*.[23]	%Diff	Casar *et al*.[37]	%Diff
6x6	0.923	0.921	-0.2	0.915	-0.9
4x4	0.867	0.865	-0.2	0.866	-0.1
3x3	0.833	0.832	-0.2	0.834	0.1
2x2	0.795	0.791	-0.6	0.793	-0.3
1x1	0.683	0.688	0.7	0.694	1.6

Many studies have found that the intermachine variability of the Varian TrueBeam™ machine is very small among different institutes.[20-22] Tanaka *et al*. [38] found a small difference of 1.0% and 1.5% when comparing the PDDs and beam profiles, respectively, between 21 TrueBeam™ machines and average data. They also reported that the deviation of the output factor of each data set from the average value was within 1.0% for the 3x3 cm^2- 30x30 cm^2 fields. These data support that the Varian phase-space file approach is feasible for MC simulation for large field because the TrueBeam™ linear accelerator data is very consistent. However, for small field, the dosimetric parameters is vary due to the difference in source size and detector selection. Akino *et al*.[36] found that the differences of the FOFs were

within ±5% for 0.5x0.5 cm^2 among 12 TrueBeam™ machines. The variation of PDD at 0.5x0.5 cm^2 was >1%. Whereas the variability <1% for 1x1 cm^2 was reported in their study. In this work, the MC results using the Varian phase-space file were compared with the published measured data from many institutions. The results revealed that our simulation agreed with other TrueBeam™ machines published data, including PDDs, beam profiles, and FOFs. Although a few studies have reported the commissioning data of Varian TrueBeam™ for small field sizes, the consistence between the MC simulation and measurement in this study indicates the excellent performance of the phase-space file for field sizes down to 1x1 cm^2. For very small field sizes (<1x1 cm^2), it is recommended that the phase-space file should be evaluated with measurement data from a given TrueBeam™ machines.

Conclusion

The Varian TrueBeam™ 6MV phase-space file version 2 released by Varian Medical System was evaluated against the measurement for small field sizes down to 0.6x0.6 cm^2. The MC simulation demonstrates good agreement with the PDDs. Although discrepancies in the inline profile were observed for field sizes ≤3x3 cm^2, it did not affect the PDD or the output factor, except for the 0.6x0.6 cm^2 field where the difference in the output factor was up to 2%. The Varian phase-space file can be used as a radiation source for accurate MC dose calculation with existing TrueBeam™ models for field sizes ≥1x1 cm^2. For very small field sizes (<1x1 cm^2) where the beam profile is strongly influenced by the source size, we recommend that the user verifies the phase-space with a specific TrueBeam™machine.

Conflicting interests

The authors declare no conflict of interest.

References

[1] PalmansH, Andreo P,Huq MS, et al. Dosimetry of small static fields used in external beam radiotherapy: an IAEA-AAPM International Code of Practice for reference and relative dose determination, Technical Report Series No. 483. International Atomic Energy Agency: Vienna, Austria, 2017.

[2] Chetty IJ, Curran B, Cygler JE, et al. Report of the AAPM Task Group No. 105: Issues associated with clinical implementation of Monte Carlo-based photon and electron external beam treatment planning. Med Phys. 2007; 34(12): 4818-53. doi: 10.1118/1.2795842.

[3] Benmakhlouf H, Sempau J, Andreo P. Output correction factors for nine small field detectors in 6 MV radiation therapy photon beams: a PENELOPE Monte Carlo study. Med Phys. 2014; 41(4): 041711. doi: 10.1118/1.4868695.

[4] Francescon P, Cora S, Satariano N. Calculation of k(Q(clin),Q(msr)) (f(clin),f(msr)) for several small detectors and for two linear accelerators using Monte Carlo simulations. Med Phys. 2011; 38(12): 6513-27. doi: 10.1118/1.3660770.

[5] Cranmer-Sargison G, Weston S, Sidhu NP, et al. Experimental small field 6MV output ratio analysis for various diode detector and accelerator combinations. Radiother Oncol. 2011; 100(3): 429-35. doi: 10.1016/j.radonc.2011.09.002.

[6] Constantin M, Perl J, LoSasso T, et al. Modeling the truebeam linac using a CAD to Geant4 geometry implementation: dose and IAEA-compliant phase space calculations. Med Phys. 2011; 38(7): 4018-24. doi: 10.1118/1.3598439.

[7] Belosi MF, Rodriguez M, Fogliata A, et al. Monte Carlo simulation of TrueBeam flattening-filter-free beams using Varian phase-space files: Comparison with experimental data. Med Phys. 2014; 41(5): 051707. doi: 10.1118/1.4871041.

[8] Gete E, Duzenli C, Milette M-P, et al. A Monte Carlo approach to validation of FFF VMAT treatment plans for the TrueBeam linac. Med Phys. 2013; 40(2): 021707. doi: 10.1118/1.4773883.

[9] Bergman AM, Gete E, Duzenli C, et al. Monte Carlo modeling of HD120 multileaf collimator on Varian TrueBeam linear accelerator for verification of 6X and 6X FFF VMAT SABR treatment plans. J Appl Clin Med Phys. 2014; 15(3): 4686. doi: 10.1120/jacmp.v15i3.4686.

[10] Qin Y, Zhong H, Wen N, et al. Deriving detector-specific correction factors for rectangular small fields using a scintillator detector. J Appl Clin Med Phys. 2016; 17(6): 379-91. doi: 10.1120/jacmp.v17i6.6433.

[11] Feng Z, Yue H, Zhang Y, et al. Monte Carlo simulation of beam characteristics from small fields based on TrueBeam flattening-filter-free mode. Radiat Oncol. 2016; 11(1): 30. doi: 10.1186/s13014-016-0601-2.

[12] Papaconstadopoulos P, Levesque IR, Aldelaijan S, et al. Modeling the primary source intensity distribution: reconstruction and inter-comparison of six Varian TrueBeam sources. Phys Med Biol. 2019; 64: 135005. doi.org/10.1088/1361-6560/ab1ccc.

[13] Kawrakow I. The EGSnrc Code System, Monte Carlo Simulation of Electron and photon Transport. NRCC Report PIRS-701. 2001.

[14] Rogers D, Walters B, Kawrakow I. BEAMnrc users manual. Nrc Report Pirs. 2009; 509: 12.

[15] Walters B, Kawrakow I, Rogers D. DOSXYZnrc users manual. Nrc Report Pirs. 2005; 794: 57-8.

[16] Low DA, Dempsey JF. Evaluation of the gamma dose distribution comparison method. Med Phys. 2003; 30(9): 2455-64. doi: 10.1118/1.1598711.

[17] Cheng JY, Ning H, Arora BC, et al. Output factor comparison of Monte Carlo and measurement for Varian TrueBeam 6 MV and 10 MV flattening filter-free stereotactic radiosurgery system. J Appl Clin Med Phys. 2016; 17(3): 100-10. doi: 10.1120/jacmp.v17i3.5956.

[18] Teke T, Duzenli C, Bergman A, et al. Monte Carlo validation of the TrueBeam 10XFFF phase–space files for applications in lung SABR. Med Phys. 2015; 42(12): 6863-74. doi: 10.1118/1.4935144.

[19] Tzedakis A, Damilakis JE, Mazonakis M, et al. Influence of initial electron beam parameters on Monte Carlo calculated absorbed dose distributions for radiotherapy photon beams. Med Phys. 2004; 31(4): 907-13. doi: 10.1118/1.1668551.

[20] Glide-Hurst C, Bellon M, Foster R, et al. Commissioning of the Varian TrueBeam linear accelerator: A multi-institutional study. Med Phys. 2013; 40(3): 031719. doi: 10.1118/1.4790563.

[21] Beyer GP. Commissioning measurements for photon beam data on three TrueBeam linear accelerators, and comparison with Trilogy and Clinac 2100 linear accelerators. J Appl Clin Med Phys. 2013; 14(1): 4077. doi: 10.1120/jacmp.v14i1.4077.

[22] Chang Z, Wu Q, Adamson J, Ren L, et al. Commissioning and dosimetric characteristics of TrueBeam system: composite data of three TrueBeam machines. Med Phys. 2012; 39(11): 6981-7018. doi: 10.1118/1.4762682.

[23] Mamesa S, Oonsiri S, Sanghangthum T, et al. The impact of corrected field output factors based on IAEA/AAPM code of practice on small-field dosimetry to the calculated monitor unit in eclipse™ treatment planning system. J Appl Clin Med Phys. 2020; 21(5): 65-75. doi: 10.1002/acm2.12855.

[24] Chang K-H, Lee B-R, Kim Y-H, et al. Dosimetric Characteristics of Edge Detector(TM) in Small Beam Dosimetry. Korean J Med Phys. 2009; 20: 191-8.

[25] Cranmer-Sargison G, Charles PH, Trapp JV,et al. A methodological approach to reporting corrected small field relative outputs. Radiother Oncol. 2013; 109(3): 350-5. doi.org/10.1016/j.radonc.2013.10.002.

[26] Francescon P, Beddar S, Satariano N, et al. Variation of kQclin,Qmsrfclin,fmsr for the small-field dosimetric parameters percentage depth dose, tissue-maximum ratio, and off-axis ratio. Med Phys. 2014; 41(10): 101708. doi: 10.1118/1.4895978.

[27] Papaconstadopoulos P, Tessier F, Seuntjens J. On the correction, perturbation and modification of small field detectors in relative dosimetry. Phys Med Biol. 2014; 59(19): 5937. doi: 10.1088/0031-9155/59/19/5937.

[28] Dwivedi S, Kansal S, Dangwal VK, et al. Dosimetry of a 6 MV flattening filter-free small photon beam using various detectors. Biomed Phys Eng. 2021; 7(4): 045004. doi: 10.1088/2057-1976/abfd80.

[29] Akino Y, Fujiwara M, Okamura K, et al. Characterization of a microSilicon diode detector for small-field photon beam dosimetry. J Radiat Res. 2020; 61(3): 410-8. doi.org/10.1093/jrr/rraa010.

[30] Das IJ, Francescon P, Moran JM, et al. Report of AAPM Task Group 155: Megavoltage photon beam dosimetry in small fields and non-equilibrium conditions. Med Phys. 2021. doi.org/10.1002/mp.15030.

[31] Kairn T, Charles PH, Cranmer-Sargison G, et al. Clinical use of diodes and micro-chambers to obtain accurate small field output factor measurements. Australas Phys Eng Sci Med. 2015; 38(2): 357-67. doi: 10.1007/s13246-015-0334-9.

[32] Azangwe G, Grochowska P, Georg D, et al. Detector to detector corrections: a comprehensive experimental study of detector specific correction factors for beam output measurements for small radiotherapy beams. Med Phys. 2014; 41(7): 072103. doi: 10.1118/1.4883795.

[33] Liu PZ, Suchowerska N, McKenzie DR. Can small field diode correction factors be applied universally? Radiother Oncol. 2014; 112(3): 442-6. doi: 10.1016/j.radonc.2014.08.009.

[34] Lechner W, Palmans H, Sölkner L, et al. Detector comparison for small field output factor measurements in flattening filter free photon beams. Radiother Oncol. 2013; 109(3): 356-60.

[35] Smith CL, Montesari A, Oliver CP, et al. Evaluation of the IAEA-TRS 483 protocol for the dosimetry of small fields (square and stereotactic cones) using multiple detectors. J Appl Clin Med Phys. 2020; 21(2): 98-110. doi.org/10.1002/acm2.12792.

[36] Akino Y, Mizuno H, Isono M, et al. Small-field dosimetry of TrueBeam(TM) flattened and flattening filter-free beams: A multi-institutional analysis. J Appl Clin Med Phys. 2020; 21(1): 78-87. doi: 10.1002/acm2.12791.

[37] Casar B, Gershkevitsh E, Mendez I, et al. A novel method for the determination of field output factors and output correction factors for small static fields for six diodes and a microdiamond detector in megavoltage photon beams. Med Phys. 2019; 46(2): 944-63. doi: 10.1002/mp.13318.

[38] Tanaka Y, Mizuno H, Akino Y, et al. Do the representative beam data for TrueBeam(™) linear accelerators represent average data? J Appl Clin Med Phys. 2019; 20(2): 51-62. doi: 10.1002/acm2.12518.